Nanoscale

Cite this: *Nanoscale*, 2012, **4**, 3040

www.rsc.org/nanoscale

COMMUNICATION

Nanoionic transport and electrochemical reactions in resistively switching silicon dioxide

Stefan Tappertzhofen,[a] Hans Mündelein,[a] Ilia Valov*[ab] and Rainer Waser[ab]

Received 21st February 2012, Accepted 21st March 2012
DOI: 10.1039/c2nr30413a

The mobility of copper ions and redox reactions of Cu at the interface with SiO_2 being directly attributed to the resistive switching effect have been studied by cyclic voltammetry (CV). The electrode kinetics of the Cu^{z+}/Cu redox reactions were analyzed suggesting the formation of both Cu^+ and Cu^{2+} species. The ion mobility shows an unexpected strong dependence on the ion concentration indicating ion–ion interactions typical for concentrated solution conditions. Based on the standard reduction potentials for Cu^{z+}/Cu we identified partial electrochemical redox reactions during oxidation and reduction. The results contribute to a detailed understanding of the resistive switching effect in Cu/SiO_2/Pt cells and provide insight into electrochemically assisted diffusion of metal cations in oxides in general.

Non-volatile Resistive Random Access Memories (RRAMs) are emerging memory devices being considered as the next generation of memories showing low power consumption, fast switching and high prospect of scalability.[1–5] In this context, the electrochemical metallization (ECM) cell is a promising candidate for RRAM devices due to its potential multibit storage and ease of fabrication.[6] The simple structure of an ECM cell consists of a working electrode (WE, *e.g.* Cu or Ag), an ion conducting thin film (*e.g.* GeSe (ref. 7) but also SiO_2 (ref. 8)) and an electrochemically inert counter-electrode (CE, *e.g.* Pt). The resistive switching effect is attributed to the electrochemical growth and dissolution of a nanoscaled Ag or Cu filament short circuiting both electrodes[6] and has been observed in various materials.[2,9] We recently reported about anodic oxidation and reduction of Cu in Cu/SiO_2/Pt cells studied by cyclic voltammetry (CV) as the prerequisite for filament formation and thus, resistive switching.[10] We elucidated that the Cu/SiO_2 system shows charge inhibited transfer characteristics and further derived the ion diffusion coefficient and ion mobility at a specific sweep rate which were found to be much higher than the extrapolated diffusion coefficients of Cu ions in SiO_2 at room temperature.[11,12] However, the ion mobility is still too small to explain resistive switching in the μs range or below. Moreover, the contribution of the ion mobility to the strong nonlinear switching kinetic in ECM cells[8,13] is yet unknown. Strukov and Williams reported on high ion mobility at elevated temperatures (up to 800 K) and high electrical fields for oxygen vacancies in TiO_2.[14] Nevertheless, resistive switching in ECM cells occurs even at very low currents (below 10 pA (ref. 15)) which is not high enough for a significant temperature increase.[16] Despite the potential temperature increase and high electric fields, other strong nonlinear effects have not been discussed in detail yet. Meanwhile, the switching kinetic may be also attributed to the very nature of electrochemical redox reactions being the preceding processes of resistive switching which has not been, however, reported to date. For instance, the contribution of ion–ion interactions and/or partial electrochemical reactions to the switching kinetics has not yet been discussed nor investigated. In addition, the identification of individual electrochemical partial reactions and their kinetics is missing, hindering the complete fundamental understanding of the processes involved during resistive switching. Hence, in order to tune the performance of practically working ECM cells the knowledge of the kinetics of these redox reactions is of high importance as well.

In this work, we report on kinetic studies specially focused on the partial Cu^{z+}/Cu redox reactions at the interface of Cu and SiO_2. Based on the position and intensity of the current peaks, we assign each electrochemical partial reaction to a specific oxidation or reduction process. We further show a remarkable dependence of the ion diffusion coefficient and thus, ion mobility on the ion concentration, being itself related to the sweep rate.

For sample fabrication we used platinized p-doped (100) silicon wafers. A 60 nm thick SiO_2 thin film was deposited by electron-beam (e-beam) evaporation at high vacuum which is acting as the ion conducting thin film. Cu top electrodes with an area of 0.008 mm^2 to 0.2 mm^2 and a thickness of 30 nm were deposited by e-beam evaporation as well. A 100 nm thick Pt layer was finally sputtered to prevent chemical oxidation of the Cu electrodes. Pattern transfer was performed by conventional UV lithography and lift-off. For the electrode kinetic studies we employed the CV technique[17] using a Keithley 6430 sub-femto remote source meter to accomplish CV sweeps with a triangular voltage signal between −2 V and 2 V and variable sweep rates ν between 2 mV s^{-1} and 3 V s^{-1}.

The resistive switching behavior of a Cu/SiO_2/Pt cell is shown by the blue curve in Fig. 1 in logarithmic scale. By limitation of the vertex potential to 2 V resistive switching is avoided and thus, oxidation and reduction of Cu species can be analyzed prior to the switching event by cyclic voltammetry (red curve). Arrows indicate

[a]*Institut für Werkstoffe der Elektrotechnik II, RWTH Aachen University, Sommerfeldstraße 24, 52064 Aachen, Germany. E-mail: tappertzhofen@iwe.rwth-aachen.de*
[b]*Peter Grünberg Institut 7, Forschungszentrum Jülich GmbH, Wilhelm-Johnen-Straße, 52425 Jülich, Germany. E-mail: i.valov@fz-juelich.de*

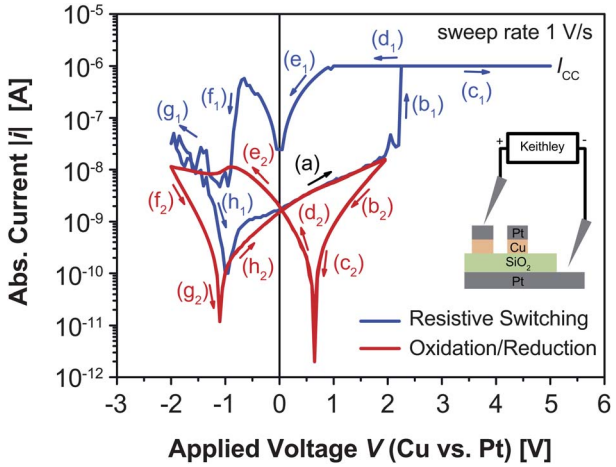

Fig. 1 Resistive switching of a Cu/SiO_2/Pt cell (blue curve). By limitation of the vertex potential resistive switching is avoided and the oxidation–reduction reactions, being the preceding processes of resistive switching, can be analyzed (red curve) by cyclic voltammetry (CV).

the sweeping direction (a) to (h) for one cycle. In the case of (a) where Cu ions are formed the red curve and blue curve are overlaid. In the cases (b) to (h) the red curve differs from the blue curve. The cell is switching at an applied voltage of approximately $V = 2.4$ V (b_1). After switching to the low resistive state a current compliance I_{CC} is used to avoid damage to the cell ((c_1) and (d_1)). The cell switches back to the high resistive state (reset) by applying a negative voltage ((f_1) to (h_1)). As mentioned above oxidation and reduction processes, which will be discussed in detail later, can be observed by the red curve ((b_2) to (h_2)) when switching is avoided. Since the current for redox processes depends on the electrode area, current densities are further plotted.

Fig. 2 depicts a typical CV sweep (linear scale) for a low sweep rate of $\nu = 15$ mV s^{-1}. By increasing the applied voltage V, anodic oxidation of the Cu electrode takes place resulting in an increase of the current. After reaching the vertex potential at $V = 2$ V the driving force for further oxidation is diminished and the current density decreases. During the following negative voltage sweep the oxidized Cu ions are reduced, whereby diffusion limitations of Cu ions injected into the SiO_2 thin film are responsible for the negative current density

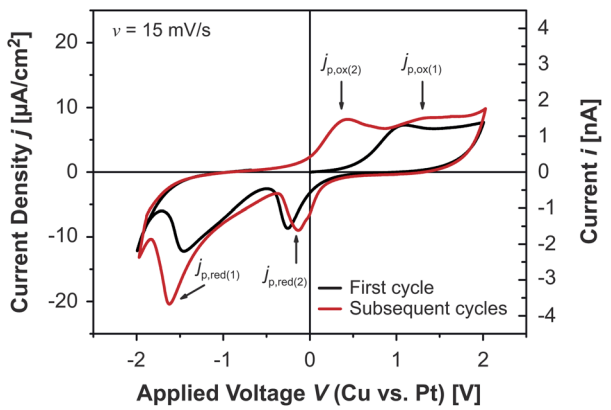

Fig. 2 Cyclic voltammetry for a Cu/SiO_2/Pt cell exemplary for a low sweep rate $\nu = 15$ mV s^{-1}. Anodic oxidation current density peaks are clearly observed.

peak $j_{p,red(2)}$.[17] The reduction of Cu at the Pt electrode can be neglected due to the voltage polarity. We contributed the subsequent reduction peak $j_{p,red(1)}$ to a partial Cu^{2+} to Cu reduction or to a partial Cu^{2+} to Cu^+ reaction.[10] In contrast to the previous study we succeeded now to observe oxidation peaks by using comparatively low sweep rates (below 34 mV s^{-1}). In this case we clearly distinguish two oxidation peaks, $j_{p,ox(1)}$ and $j_{p,ox(2)}$, as shown in Fig. 2. Note, peak $j_{p,ox(2)}$ is only observed for subsequent cycles but not observed during the first sweep when the cell is in an initial state. Moreover, $j_{p,ox(1)}$ and $j_{p,ox(2)}$ cannot be clearly observed by the increase of ν above ~25 mV s^{-1} which will be discussed later.

An appropriate reference electrode typically used to analyze CV curves cannot be used in our thin film geometry making it difficult to easily identify electrochemical reactions. Since the charge number z of Cu^{z+} ions in resistively switching SiO_2 is yet unknown the interpretation of $j_{p,ox(1)}$ and $j_{p,ox(2)}$ as well as $j_{p,red(1)}$ and $j_{p,red(2)}$ can lead to the identification of each electrochemical partial reaction. In aqueous solutions the standard redox potentials for Cu are given as: Cu^+/Cu ($E^{\varphi,1} = 0.52$ V), Cu^{2+}/Cu ($E^{\varphi,2} = 0.34$ V) and Cu^{2+}/Cu^+ ($E^{\varphi,3} = 0.159$ V).[18] Although Cu ions are dissolved in SiO_2 in this case, the general trend of reduction potentials holds here as well and furthermore, incorporation of water in SiO_2 based ECM cells has been reported.[19,20] Thus, Cu should be oxidized to Cu^{2+} first since this process is thermodynamically favorable according to the standard redox potentials. We attribute the current density peak $j_{p,ox(1)}$ to this partial reaction. The Cu to Cu^+ oxidation takes place after $j_{p,ox(1)}$ and a current density peak may be beyond the vertex potential of 2 V. Hence, both Cu^+ and Cu^{2+} can be found in SiO_2 after the oxidation. When V is decreased the reduction of Cu^+ to Cu is thermodynamically favorable (lower reduction energy) resulting in the current density peak $j_{p,red(2)}$. The absolute current density increases further close to the vertex potential −2 V which is an indication for Cu^{2+} to Cu reduction ($j_{p,red(1)}$) and by a further decrease of V Cu^{2+} to Cu^+ reduction may take place as well. When a subsequent cycle is started a new $j_{p,red(2)}$ oxidation peak is observed. Considering that only a part of the generated Cu^+ ions were reduced these ions can now undergo oxidation to Cu^{2+} ions since the standard reduction potential for this process is lower than for Cu to Cu^+ or Cu^{2+}.

Thus, during the first sweep cycle Cu^{2+} ions are produced according to CV measurements. Cu^+ ions seem to be formed at higher positive voltages close to the switching voltage and also during reduction sweep. The subsequent cycles clearly indicate the presence of Cu^+ which can contribute to filament formation. Since the switching event takes place after the Cu^{2+} formation Cu^+ ions generated beyond the vertex potential may be the dominating species for resistive switching. However, for a comprehensive theoretical model of the switching kinetics both ion species need to be considered.

For simplification we assume that Cu^+ is the dominating ion and thus, $z = 1$. Now, the Cu^{z+} ion concentration c_{ox} can be estimated by integration of the current during anodic oxidation (depicted in Fig. 3(a) for $\nu = 34$ mV s^{-1}) and cell geometry as reported in ref. 10 for a specific sweep rate $\nu = 160$ mV s^{-1}. We found that c_{ox} depends on ν as depicted in Fig. 3(b). The ion concentration decreases by increasing ν which we attribute to a shorter time for oxidation during the sweep for high values of ν. At low sweep rates sufficient time is available for oxidation of Cu and thus c_{ox} is increased. The diffusion coefficient of Cu ions can be calculated using the Randles–Sevcik equation:[17]

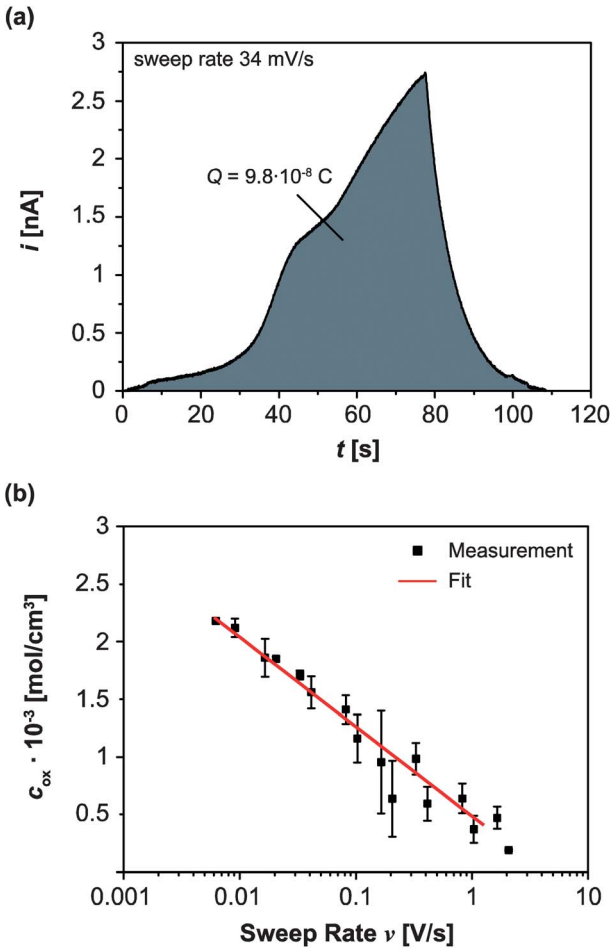

Fig. 3 Estimated Cu^{z+} concentration c_{ox} after anodic oxidation. (a) Integration of current during oxidation exemplary for $\nu = 34$ mV s^{-1}. The estimated charge of oxidized Cu ions is about $Q = 98$ nC. (b) Cu^{z+} concentration c_{ox} *versus* sweep rate ν. c_{ox} decreases by the increase of the sweep rate.

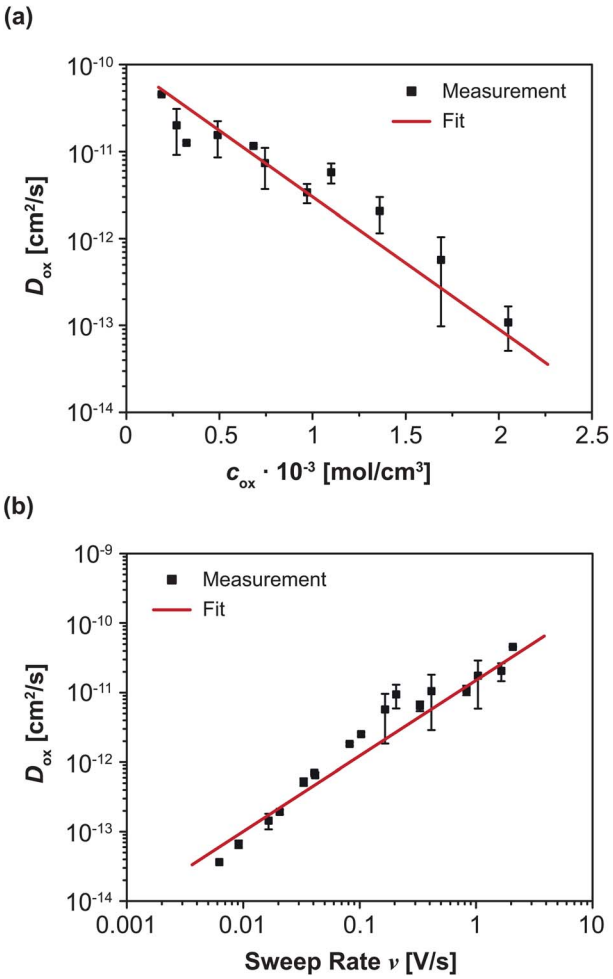

Fig. 4 Calculated diffusion coefficient D_{ox} of Cu^{z+} ions *versus* ion concentration (a) and sweep rate ν (b). As the Cu^{z+} ion concentration seems to decrease by the increase of ν the diffusion and thus the mobility of Cu^{z+} increases.

$$j_{p,red} = 2.99 \times 10^5 \cdot z^{3/2}\, c_{ox} \sqrt{\alpha D_{ox} \nu} \qquad (1)$$

Here, D_{ox} is the diffusion coefficient of the Cu^{z+} in cm^2 s^{-1}, z the number of electrons transferred in the redox reaction, c_{ox} the concentration in mol cm^{-3}, $\alpha \approx 0.5$ the charge transfer coefficient and ν the sweep rate in V s^{-1}. $j_{p,red}$ (in A cm^{-2}) is the absolute reduction current density peak assuming that the reduction of Cu^+ ($z = 1$) is dominating. The estimation of D_{ox} is complicated when more than one reduction current density peak is clearly observed (below $\nu = 34$ mV s^{-1}). In this case the dominating peak is used for a first approximation of D_{ox}.

For most of the ion conducting solids the ion mobility is expected to be nearly independent of the defect concentration presuming an ideally diluted solution. In contrast, we observed a strong dependence of the diffusion coefficient of Cu^{z+} ions on c_{ox} (Fig. 4(a)). By decreasing the sweep rate the ion concentration is increased and D_{ox} decreases indicating that the SiO_2 layer close to the Cu electrode behaves as a concentrated solution. Thus, ion–ion interactions cannot be neglected which result in a decrease of D_{ox}. At high sweep rates, less time is available for Cu oxidation and c_{ox} is low. The fewer ion–ion interactions result in an increase of D_{ox} and thus, the ion mobility.

The dependence of D_{ox} on ν depicted in Fig. 4(b) can also explain why current density peaks for anodic oxidation are clearly observed when decreasing the sweep rate. Here, the high ion concentration decreases D_{ox} and further oxidation is limited by the diffusion of Cu^{z+} into SiO_2. At high sweep rates the fewer oxidized ions can diffuse faster in SiO_2 and the diffusion limitation is less pronounced.

Although the previously reported D_{ox} is much higher than extrapolated diffusion coefficients of Cu ions in SiO_2 at room temperature it is still too small to explain resistive switching in the µs regime or below in the case of pulse measurements.[10] However, this study reveals that D_{ox} can be even further increased at high sweep rates. This is much closer to the case of pulse measurements where the time for oxidation is short resulting in a higher ion diffusion coefficient and thus, faster filament growth.

In conclusion we reported on partial Cu^{z+}/Cu half-cell redox reactions at the interface with SiO_2 with special attention paid to the kinetics of ion mobility. We found that close to the Cu electrode SiO_2 acts as a concentrated solution which impacts the Cu^{z+} diffusion coefficient D_{ox} and thus the ion mobility. At higher sweep rates ν we estimated a higher ion diffusion coefficient, which is significantly reduced for low sweep rates. Based on the position and the sequence

of the current density peaks for oxidation and reduction in the cyclic voltammogram we identified the partial electrochemical redox reactions of Cu at the interface with SiO_2 demonstrating that both Cu^+ and Cu^{2+} are involved during voltage sweeping. These effects contribute to the strong nonlinear switching kinetics reported for SiO_2. The results account for the development of a comprehensive theory of the resistive switching effect in $Cu/SiO_2/Pt$ cells and in general for other oxide based electrochemical metallization cells.

Notes and references

1 R. Waser and M. Aono, *Nat. Mater.*, 2007, **6**, 833–840.
2 Y. Fujisaki, *Jpn. J. Appl. Phys.*, 2010, **49**, 1–14.
3 K. Terabe, T. Hasegawa, T. Nakayama and M. Aono, *Nature*, 2005, **433**, 47–50.
4 A. Geresdi, A. Halbritter, A. Gyenis, P. Makk and G. Mihaly, *Nanoscale*, 2011, **3**, 1504–1507.
5 D. B. Strukov, G. S. Snider, D. R. Stewart and R. S. Williams, *Nature*, 2008, **453**, 80–83.
6 I. Valov, R. Waser, J. R. Jameson and M. N. Kozicki, *Nanotechnology*, 2011, **22**, 254003.
7 M. Mitkova and M. N. Kozicki, *J. Non-Cryst. Solids*, 2006, **352**, 567–577.
8 Y. Bernard, V. T. Renard, P. Gonon and V. Jousseaume, *Microelectron. Eng.*, 2011, **88**, 814–816.
9 M. N. Kozicki, C. Gopalan, M. Balakrishnan and M. Mitkova, *IEEE Trans. Nanotechnol.*, 2006, **5**, 535–544.
10 S. Tappertzhofen, S. Menzel, I. Valov and R. Waser, *Appl. Phys. Lett.*, 2011, **99**, 203103.
11 J. D. McBrayer, R. M. Swanson and Y. W. Sigmon, *J. Electrochem. Soc.*, 1986, **133**, 1242–1246.
12 Y. Shacham-Diamand, A. Dedhia, D. Hoffstetter and W. G. Oldham, *J. Electrochem. Soc.*, 1993, **140**, 2427–2432.
13 S. Menzel, B. Klopstra, C. Kügeler, U. Böttger, G. Staikov and R. Waser, *Mater. Res. Soc. Symp. Proc.*, 2009, **1160**, 101–106.
14 D. B. Strukov and R. S. Williams, *Appl. Phys. A: Mater. Sci. Process.*, 2009, **94**, 515–519.
15 C. Schindler, M. Weides, M. N. Kozicki and R. Waser, *Appl. Phys. Lett.*, 2008, **92**, 122910.
16 S. Menzel, M. Waters, A. Marchewka, U. Böttger, R. Dittmann and R. Waser, *Adv. Funct. Mater.*, 2011, **21**, 4487.
17 A. Bard and L. Faulkner, *Electrochemical Methods: Fundamentals and Applications*, John Wiley and Sons, 2001.
18 A. J. Bard, J. Jordan and R. Parsons, *IUPAC Recommendations*, 1985.
19 T. Tsuruoka, K. Terabe, T. Hasegawa, I. Valov, R. Waser and M. Aono, *Adv. Funct. Mater.*, 2011, **22**, 70.
20 S. Tappertzhofen, M. Hempel, I. Valov and R. Waser, *Mater. Res. Soc. Symp. Proc.*, 2011, **13**, 1.